

A Numerical Investigation of Continuous Wave Parametric Gain in Silicon Nano-Waveguides at Wavelengths around 1550 nm

Giannino Dziallas^{1*}, Mahmoud Jazayerifar¹, Andrzej Gajda², Lars Zimmermann², Klaus Petermann¹

¹ Institut für Hochfrequenz- und Halbleiter-Systemtechnologien, Technische Universität Berlin, D-10587 Berlin, Germany

² IHP, Im Technologiepark 25, D-15232 Frankfurt (Oder), Germany

* Giannino@mail.tu-berlin.de

Abstract— We developed a numerical model to investigate continuous wave four wave mixing (FWM) in silicon nano-waveguides with embedded PIN junctions. The model is complemented by fitting to the experimental data. Using the model we show that the FWM gain in silicon can compensate for all relevant loss mechanisms (two photon and free carrier absorption as well as linear loss) provided that the carrier lifetime is low enough (few tens of picoseconds).

Keywords-- parametric amplification, four-wave-mixing, silicon waveguide, pin-junction

I. INTRODUCTION

Silicon nano-waveguides for nonlinear signal processing have attracted a lot of attention, due to the ultrafast optical Kerr effect and high confinement leading to a nonlinear coefficient that is almost four orders of magnitude larger than in highly nonlinear fibres. Having continuous wave (cw) gain in silicon waveguides is the enabling step for optical signal processing on a centimetre length scale [1]. So far no cw parametric gain at wavelengths around 1550 nm has been shown in silicon, mostly due to the impairing effect of two photon absorption (TPA) loss and free carrier absorption (FCA) existing in silicon. We have recently shown that the four-wave mixing (FWM) efficiency can be significantly enhanced by embedding a reversed biased pin junction in a silicon waveguide to sweep out the generated carriers [2] as shown schematically in Fig. 1.

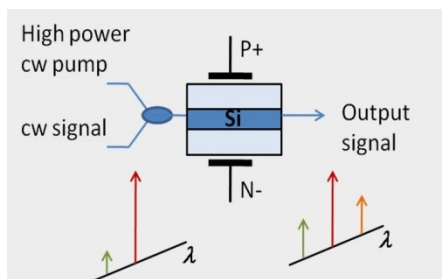


Fig. 1. The schematic of FWM gain experiment

In this paper we develop a nonlinear propagation model including the Kerr effect, TPA and carrier-related effects to investigate the cw parametric gain in the silicon waveguide. After fitting the simulation results to the measured signal-idler conversion efficiency (CE), we discuss the cw FWM gain in silicon. The rest of this paper is as follows: In section II the numerical model is introduced. In section III the numerical values which are used in the model are obtained. In section IV the model is used to discuss the FWM gain process in silicon waveguides.

II. NUMERICAL MODEL

The nonlinear propagation in silicon is modelled by the nonlinear Schrödinger equation (NLSE), taking into account the linear and nonlinear TPA losses, the Kerr effect, chromatic dispersion and free-carrier effects through an additional loss and refractive index change. The following equation is solved numerically using the symmetrical split step Fourier method:

$$\frac{\partial A}{\partial z} = \left(-\frac{\alpha_{lin}}{2} - \frac{\alpha_{FC}}{2} \right) A - \sum_{n=1}^{\infty} \frac{j^{n-1} \cdot \beta_n}{n!} \cdot \frac{\partial^n A}{\partial t^n} + \left(j\gamma - \frac{\alpha_{TPA}}{2} \right) |A|^2 A - j \frac{2\pi}{\lambda} \Delta n_{FC} A$$

Where A , j , α_{lin} , α_{FC} , α_{TPA} , β_n , γ , λ and Δn_{FC} are the complex amplitude, unit imaginary number, linear absorption, free-carrier absorption, two-photon absorption, n -th order dispersion coefficient, nonlinear kerr coefficient, wavelength and the index change caused by the generated free carriers, respectively. In cw operation the values of γ , α_{TPA} , α_{FC} , Δn_{FC} and β_n are calculated as follows:

$$\gamma = \Gamma \cdot \frac{2\pi}{\lambda} \frac{n_2}{A_{eff}}, \quad \alpha_{TPA} = \Gamma \cdot \frac{\beta_{TPA}}{A_{eff}}$$

$$\alpha_{FC} = \sigma_{FC} \cdot N(z), \quad \Delta n_{FC} = -\zeta_{FC} \cdot N(z)$$

$$N(z) = \frac{\beta_{TPA}}{2\hbar\omega} \cdot \tau_{eff} \cdot I(z)$$

where σ_{FC} is the free-carrier absorption cross-section, ζ_{FC} is the free-carrier index coefficient, $N(z)$ is the steady-state carrier density along the waveguide, τ_{eff} is the effective free-carrier lifetime, β_{TPA} is the TPA coefficient, $I(z)$ is the intensity along the waveguide, \hbar is the Planck's constant, ω is the optical frequency, A_{eff} is the effective area, n_2 is the nonlinear Kerr coefficient and Γ is a nonlinear enhancement factor due to the high-confinement inside the waveguide [8].

III. NUMERICAL VALUES FOR THE MODEL

Different measured values for the nonlinear coefficients of silicon around the telecom wavelength 1.55 μm have been reported by different groups, which are partly listed in table I. There is a considerable difference in the measured values, leading to different effective nonlinear coefficients γ and different FWM efficiencies. Employing different values of table I in our numerical model, we choose those values which fit to our previously reported measurements [2] the best.

TABLE I
MEASURED NONLINEAR COEFFICIENTS [3] AND CALCULATED γ

Affiliation	n_2 (cm^2W^{-1}) $\times 10^{-13}$	β_{TPA} (cmW^{-1}) $\times 10^{-9}$	γ ($\text{cm}^{-1}\text{W}^{-1}$) (incl. enhancement factor Γ)
CUHK	0.60	0.45	2.8
UBC	0.70	0.90	3.3
Bell	0.45	0.79	2.1
NEC	1.45	0.60	6.8

A SOI nano-rib waveguide with the dimensions $H = 220\text{nm}$, slab height $s = 50\text{nm}$, rib width $w = 500\text{nm}$, length $L = 4\text{ cm}$ and with an embedded pin junction was used in the experiment [2]. Fig. 2 shows the conversion efficiency (CE, the ratio of the output idler power to the output signal power) versus wavelength. Both experimental and numerical results are shown. A good agreement between the simulation and experiment is obtained by considering a linear loss of 1 dB/cm, a dispersion coefficient of $-2450\text{ ps}/(\text{nm}\cdot\text{km})$, $\sigma_{\text{FC}}=1.45\times 10^{-21}\text{ m}^{-2}$ and $\zeta_{\text{FC}}=5.3\times 10^{-27}\text{ m}^{-3}$ [4] and a coupling loss of 3.1 dB [5]. The effective lifetimes of $\tau_{\text{eff}}=20\text{ ps}$ and $\tau_{\text{eff}}=4.5\text{ ns}$ correspond to a reverse bias of 28 V and 0 V respectively. Effective carrier lifetimes without PIN junction are usually in the nano-to millisecond range [1], but a reduction of lifetimes down to 10 ps have been measured in a silicon waveguide with PIN junction [6], with potential for an even further reduction down to 3 ps [7].

It is important to note that we achieved the best fit in our numerical CE simulations with the lowest Kerr coefficients from table I: $n_2=0.45\times 10^{-13}\text{ cm}^2\text{W}^{-1}$ and $\beta_{\text{TPA}}=0.79\times 10^{-13}\text{ cm}^2\text{W}^{-1}$. Using these values we calculate a γ of $2.1\text{ W}^{-1}\text{cm}^{-1}$ for our waveguide considering the enhancement factor of $\Gamma=1.9$ because of the high confinement and a lower group velocity [8]. This γ value is used in the following simulations of parametric amplification.

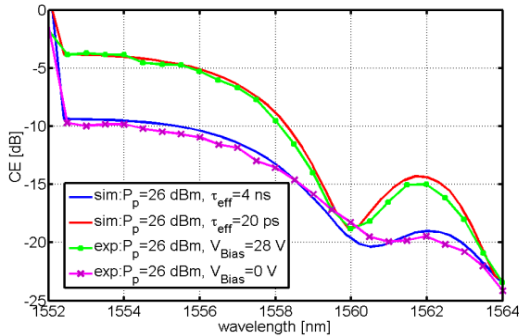


Fig. 2. Conversion efficiency of the output idler to output signal as a function of the signal wavelength. Pump power at the grating is 26 dBm, signal power at the grating is -10 dBm, pump wavelength is 1552 nm. Experimental results are shown by lines with markers.

IV. CW PARAMETRIC GAIN

Using our numerical model, we have plotted the signal loss versus the waveguide length in Fig. 3. We have assumed a pump and signal wavelength of 1552 nm and 1548 nm, respectively. The coupling losses are neglected and the pump power levels, which are specified in the figure, are the power levels at the input of the waveguide. The input signal power is -10 dBm. The carrier lifetime is 20 ps (corresponding to a reverse bias voltage of 28 V) and the linear loss is 1 dB/cm. The dispersion is $-500\text{ ps}/(\text{nm}\cdot\text{km})$ which is easily realizable

with a silicon waveguide. The rest of the numerical values are as specified in section III.

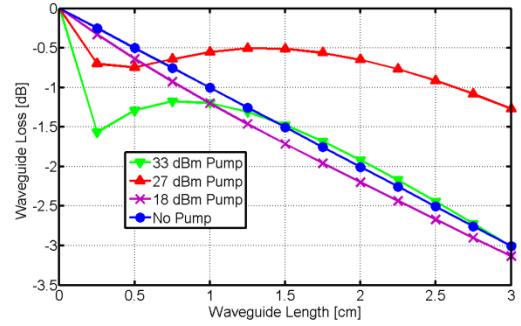


Fig. 3. Simulation results for the waveguide loss versus the length of the waveguide for different pump powers (carrier lifetime=20 ps, linear loss=1 dB/cm, dispersion=-500 ps/(nm·km), pump wavelength=1552 nm, signal wavelength=1448 nm)

If we compare the case of no-pump with the case of 18 dBm pump, we observe that the loss is increased after applying the pump. The reason is that the 18 dBm pump increases the TPA and FCA losses, while it is not strong enough to start an efficient FWM process. In the case of 27 dBm pump, we observe that at short propagation distances (lengths $< 0.5\text{ cm}$) the loss increases due to the increase of TPA and FCA losses. However, after a certain propagation distance the FWM gain overcomes these losses such that the waveguide loss with the 27 dBm pump is less than the waveguide loss without the pump. The reason is that the FWM at the input of the waveguide is not efficient since no idler is present at the input, but after certain propagation distance a phase matched idler is generated which leads to an efficient FWM which is able to overcome the losses. Judging from the 27 dBm curve, real positive phase sensitive parametric gain in silicon should be feasible since the idler is also present at the input in the case of phase sensitive operation. For the 33 dBm pump the FCA and TPA losses are so high that the FWM gain can not overcome the losses. Therefore, the pump power should be optimized to achieve the maximum FWM efficiency. Needless to say that the FWM efficiency can even be further increased if a waveguide with a less linear loss ($< 1\text{ dB/cm}$) and a lower carrier lifetime ($< 20\text{ ps}$) is implemented.

V. CONCLUSION

Using our experimentally verified model, we showed that the FWM gain in silicon can overcome the TPA and FCA losses in case the pump power is optimized and the carrier lifetime is reduced down to few tens of picoseconds by the reverse biased PIN junction. We estimate an optimum pump power of $\sim 27\text{ dBm}$ for a silicon waveguide with linear loss of 1 dB/cm.

REFERENCES

1. J. Leuthold, et al. Nat. Photonics **4**, 535 (2010).
2. A. Gajda et al, Opt. Express **20**, 13100 (2012).
3. P. Dumon et al, Jpn. J. Appl. Phys. PART 1-Regul. Pap. BRIEF Commun. Rev. Pap. **45**, 6589 (2006).
4. I. D. Rukhlenko et al, IEEE J. Sel. Top. Quantum Electron. **16**, 200 (2010).
5. H. Tian et al, J. Eur. Opt. Soc.-Rapid Publ. **7**, (2012).
6. A. C. Turner-Foster et al, Opt. Express **18**, 3582 (2010).
7. A. Gajda et al, Opt. Express **19**, 9915 (2011).
8. V. Shahraam Afshar et al, Opt. Express **21**, 18558 (2013).
9. W. Mathlouthi et al, Opt. Express **16**, 16735 (2008).
10. Y.-H. Kuo et al, Opt Express **14**, 11721 (2006).